Title

Ecosystem groundwater use enhances carbon assimilation and tree growth in a semi-arid Oak Savanna

Authors

Ruehr, Sophie

Girotto, Manuela

Verfaillie, Joseph G

et al.

Publication Date

2023-11-01

DOI

10.1016/j.agrformet.2023.109725

Agricultural and Forest Meteorology 342 (2023) 109725

Contents lists available at ScienceDirect

Agricultural and Forest Meteorology

journal homepage: www.elsevier.com/locate/agrformet

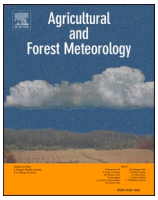

Ecosystem groundwater use enhances carbon assimilation and tree growth in a semi-arid Oak Savanna

Sophie Ruehr [a,b,*], Manuela Girotto [a], Joseph G. Verfaillie [a], Dennis Baldocchi [a], Antione Cabon [c], Trevor F. Keenan [a,b]

[a] UC Berkeley Department of Environmental Science, Policy and Management, Berkeley, CA, USA
[b] Lawrence Berkeley National Laboratory Earth Sciences Division, Berkeley, CA, USA
[c] Swiss Federal Research Institute for Forest, Snow and Landscape Research WSL, Birmensdorf, Switzerland

ARTICLE INFO

Keywords:
Groundwater
Carbon cycling
Plant hydraulics
Dendrochronology
Machine learning

ABSTRACT

Ecosystem reliance on groundwater, defined here as water stored in the saturated zone deeper than one meter beneath the surface, has been documented in many semi-arid, arid, and seasonally-dry regions around the world. In California, groundwater sustains ecosystems and mitigates mortality during drought. However, the effect of groundwater on carbon cycling still remains largely unresolved. Here we use 20 years of eddy covariance, groundwater, and tree growth measurements to isolate the impact of groundwater on carbon cycling in a semi-arid Mediterranean system in California during the summer dry season. We show that daily ecosystem groundwater use increases under positive groundwater anomalies and is associated with increased carbon assimilation and evapotranspiration rates. Negative groundwater anomalies result in significantly reduced ecosystem groundwater uptake, gross primary productivity, and evapotranspiration, with a simultaneous increase in water use efficiency. Three machine learning algorithms better predict gross primary productivity and tree growth anomalies when trained using groundwater data. These models suggest that groundwater has a unique effect on carbon assimilation and allocation to woody growth. After controlling for the effect of soil moisture, which is often decoupled from groundwater dynamics at the site, wet groundwater anomalies increase canopy carbon assimilation by 179.4 ± 25.7 g C m^{-2} (17 % of annual gross primary productivity) over the course of the summer season relative to dry groundwater anomalies. Similarly, annual tree growth increases by 0.175 ± 0.035 mm (17.7 % of annual growth) between dry and wet groundwater anomalies, independent of soil moisture dynamics. Our results demonstrate the importance of deep subsurface water resources to carbon assimilation and woody growth in dryland systems, as well as the benefits of collocated, long-term eddy covariance and ancillary datasets to improve understanding of complex ecosystem dynamics.

Key points

Long-term eddy covariance flux and ancillary data enable detection of ecosystem reliance on groundwater

High rates of ecosystem groundwater use correspond to increased evapotranspiration and carbon assimilation

Observations of groundwater anomalies improve machine learning algorithm prediction of carbon assimilation and tree growth

Wet groundwater conditions directly increased annual carbon assimilation and tree growth increased by 19.9 % and 17.7 %, respectively, compared to dry conditions

Data availability

Tonzi Ranch eddy covariance flux tower and groundwater datasets are available through the AmeriFlux server at https://ameriflux.lbl.gov/doi/AmeriFlux/US-Ton/. Dendrochronology data are available at https://datadryad.org/stash/dataset/doi:10.5061/dryad.15dv41nzt. Additional groundwater data spanning 2000-2022 from a Calfironia Department of Water Resources well (#07N08E36B001M) are available at https://wdl.water.ca.gov/. Reconstructed terrestrial water storage time series are available at

* Corresponding author at: UC Berkeley Department of Environmental Science, Policy and Management, Berkeley, CA, USA.
E-mail address: sophie_ruehr@berkeley.edu (S. Ruehr).

https://doi.org/10.1016/j.agrformet.2023.109725
Received 21 February 2023; Received in revised form 11 September 2023; Accepted 21 September 2023
Available online 16 October 2023

http://doi.org/10.5905/ethz-1007-85. TerraClimate historic monthly climate and climatic water balance data are available at https://doi.org/10.7923/G43J3B0R.

1. Introduction

Access to groundwater by plants is often ignored by earth system models that compute fluxes of water and carbon. Since 1900, terrestrial ecosystems have sequestered enough carbon via photosynthesis to avoid 85 ppm (187 Pg) of additional atmospheric CO_2 and 0.3 °C of warming (Shevliakova et al., 2013). The strength of the terrestrial carbon sink is limited by water resources, like soil moisture, which can become depleted during drought (Green et al., 2019; Stocker et al., 2018). Many terrestrial ecosystems rely also on groundwater, which is water stored in the saturated zone, typically greater than one meter (m) below the surface in dryland systems, or in fractured bedrock. Groundwater is often recharged by subsurface lateral flow and can become decoupled from shallower soil moisture in the vadose zone (<1 m deep) (Maxwell et al., 2014). Therefore, groundwater may provide an alternative water source to vegetation during drought, allowing terrestrial ecosystems to survive and continue assimilating carbon even under dry soil moisture conditions (Chitra-Tarak et al., 2021; Neumann and Cardon 2012; Yan and Dickinson 2014; Meyers et al., 2021; Baldocchi et al., 2021).

Climate change is increasing the frequency and intensity of extreme weather events, including regional drought in the western United States (Zhang et al., 2021). Drought diminishes the ability of vegetation to sequester carbon, resulting in a positive feedback to climate change (Anderegg et al., 2015; Xu et al., 2019), especially in semi-arid regions, where ecosystems are highly sensitive to soil water availability (Li et al., 2022). As semi-arid regions account for a large portion of inter-annual variability in the terrestrial carbon sink, improved understanding of groundwater reliance in semi-arid systems will benefit carbon cycle modeling (Ahlström et al., 2015; Humphrey et al., 2018), as well as understanding ecosystem responses to drought (Mu et al., 2021) and mortality events (Goulden and Bales 2019; Kibler et al., 2021).

Access to groundwater depends largely on below-ground structure, including bedrock fracturing, impermeable clay layers, and soil characteristics. Rooting depth and distribution, for example, determines access to subsurface water resources and is highly correlated with climate (Tumber-Dávila et al., 2022; Canadell et al., 1996). Semi-arid, arid and seasonally-dry climates maintain greatest maximum rooting depths (Fan et al., 2017; Canadell et al., 1996). Although the majority of roots are constrained to the top 2 m of the soil column in many systems (Jackson et al., 1996), a small but important fraction of plant roots exceeds 2 m and may extend to >60 m in some regions (Fang et al., 2017; Yang et al., 2016; Canadell et al., 1996), allowing plants to tap into deep water sources during drought (Chitra-Tarak et al., 2021; McCormick et al., 2021). Deep tap roots have up to 38 times greater hydraulic conductivity than shallow roots and can efficiently redistribute large volumes of water upwards (McElrone et al., 2004). Plant hydraulic redistribution between deep and shallow roots maintains plant functionality during periods of water stress (Mu et al., 2021) or dry seasons (Neumann and Cardon 2012) and may benefit the water and nutrient budget of entire ecosystems (Burgess et al., 1998). Recent work has even suggested that 37 % of vegetated surfaces on Earth access water resources >2 m deep (Stocker et al., 2023). However, rooting behavior remains exceedingly challenging to quantify over larger spatial extents, with different methods suggesting divergent estimates of rooting depth (Liu et al., 2021; Stocker et al., 2023).

Remote sensing and eddy covariance flux data have been used to examine ecosystem dependence on groundwater and how these relationships depend on plant hydraulic traits (Thompson et al., 2011; Orellana et al., 2012; Anderegg et al., 2018, 2020; Ma et al., 2016). Terrestrial water storage, a proxy of total water in the soil column including groundwater, influences growing season dynamics (Geruo et al., 2020), and many regions in the continental United States with shallow soils regularly use water stored in fractured bedrock (McCormick et al., 2021). Mass forest mortality events in the Sierra Nevada have also been linked to long term depletion of groundwater resources (Goulden and Bales 2019), suggesting widespread use of bedrock water in mitigating drought-induced mortality. Groundwater data collected at high temporal resolution suggest ecosystem reliance on groundwater comprises a significant portion of evapotranspiration (ET) in seasonally-dry sites (Butler et al., 2007; Steven et al., 2005; Miller et al., 2010; Ridolfi et al., 2006; Baldocchi et al., 2021). Previous studies that parameterized groundwater in models found groundwater influences evapotranspiration rates, with an increase in evapotranspiration (Lee et al., 2005; Maxwell and Condon 2016), and optimizing rooting depth can improve terrestrial biosphere model predictions of carbon assimilation rates (Kleidon and Heimann, 1998b). ET increased by ~40 %, with a simultaneous increase in ecosystem productivity, over the Amazon when hydraulic redistribution was parameterized in coupled atmospheric circulation and hydrology models (Lee et al., 2005; Maxwell and Condon 2016). However, coupling groundwater and land surface models is computationally costly and to date has been accomplished only at regional scales (Maxwell and Condon 2016).

Ecosystem reliance on groundwater specifically for carbon assimilation and woody growth remains highly uncertain. Groundwater-vegetation relationships are challenging to quantify due to a dearth of reliable groundwater datasets, long term records, and rooting depth measurements (Dawson et al., 2020). Therefore, groundwater-vegetation dynamics are typically not included in most global climate models and reanalysis systems (Roebroek et al., 2020). For example, in MERRA-2, a global reanalysis system that provides gridded estimates of land surface and atmospheric variables, the rooting zone is constrained to 1 m depth, precluding meaningful representation of groundwater-vegetation relationships, which may occur much deeper underground (Draper et al., 2018; Gelaro et al., 2017; ; Kleidon and Heimann, 1998a, 1998b). Furthermore, groundwater-vegetation dynamics vary over space by plant functional type, landscape positioning, and underlying soil, water table and bedrock structure (Geruoa et al., 2015; Roebroek et al., 2020; Koirala et al., 2017; Fang et al., 2017), resulting in heterogeneity that poses challenges for quantifying terrestrial ecosystem dependence on groundwater across spatial scales (Dawson et al., 2020; McCormick et al., 2021). In addition, most studies regarding groundwater-vegetation relationships have relied on static maps of water table depth (WTD, the depth below the surface of the saturated aquifer) that do not account for inter-annual variation in groundwater availability (Roebroek et al., 2020; Koirala et al., 2017). WTD varies seasonally and from year to year, which may determine whether plants can access water resources (McCormick et al., 2021). Another challenge is delineating the effect of groundwater from soil moisture, both of which are highly coupled in many ecosystems. Finally, few studies have explicitly considered how groundwater conditions affect carbon assimilation rates and long-term carbon sequestration in vegetation; therefore, the effect of groundwater on the carbon cycle remains largely unresolved.

In this study, we synthesize several independent data streams from Tonzi Ranch, an AmeriFlux core site (US-Ton), which has been operational since 2001. Measuring fluxes over a semi-arid woody savanna in the foothills of the Californian Sierra Nevada, US-Ton is a well-instrumented site that is representative of the region, where collocated groundwater, tree growth, and eddy covariance flux tower data provide an opportunity to explore dynamics between groundwater and ecosystem carbon cycling. The long-term dataset offers an opportunity to examine ecosystem dependence on groundwater independent from soil moisture dynamics, which have been inferred but not explicitly quantified at the site in previous studies.

We hypothesize that plant-accessible groundwater sustains ecosystem function under soil moisture drought. We expect that

enhanced groundwater-derived transpiration corresponds to less conservative water use strategies in which the ecosystem fixes more carbon while maintaining lower water use efficiency. We also expect that groundwater measurements will improve model predictions of carbon fixation and respiration and tree growth rates. Finally, we hypothesize positive groundwater anomalies and increased groundwater use will increase carbon assimilation and respiration and tree growth relative to groundwater drought.

2. Site description

Tonzi Ranch is a Mediterranean oak savanna in the foothills of the Sierra Nevada, California. The site is dominated by blue oak (*Quercus douglasii*) and some gray pine (*Pinus sabiniana*) (Osuna et al., 2015). The under story is a mixture of C3 grasses (*Brachypodium distachyon, Hypochaeris glabra, Bromus madritensis*) that green during the rainy season in the winter (November-March). These grasses desiccate as soil moisture is depleted over the course of the dry season, which typically spans May to October. The shallow soil (< 1 m) is underlain by fractured bedrock (Koteen et al., 2015), which stores water that trees access through deep tap roots (Miller et al., 2010; McCormick et al., 2021). Older and larger trees at Tonzi maintain a narrow, deep rooting system, suggesting root penetration through bedrock (Raz-Yaseef et al., 2013). The mean depth to the saturated zone (i.e., water table depth, WTD) at Tonzi Ranch is –8 m below the surface, with a range of –10.9 to –2.2 m over the course of the time series (2001-present, Fig. S1). Anthropogenic, tidal, atmospheric pressure, and temperature effects were previously determined to have little effect on diel groundwater variations at the site (Miller et al., 2010). The aquifer is recharged by a combination of precipitation and lateral flow from snow melt in the Sierra (Ma et al., 2016).

Booms and busts in rainfall have resulted in a system well-adapted to seasonal drought (Ma et al., 2016). Groundwater-derived transpiration has been documented at the site: on average 87 mm of 420 mm (21 %) of total annual ET is derived from groundwater (Baldocchi et al., 2021). Isotope studies at the site suggest >80 % of evapotranspiration is derived from subsurface waters during the dry summer months (Miller et al., 2010), and groundwater controls leaf water potentials throughout the dry season (Osuna et al., 2015). Tonzi Ranch is representative of other groundwater-dependent ecosystems throughout Mediterranean California (Kirchner et al., 2020; Klos et al., 2018; Dawson et al., 2020; Meyers et al., 2021), presenting a unique opportunity to isolate the effect of groundwater on regional carbon cycling.

3. Data and methods

3.1. Data collection & processing

Eddy covariance measurements collected at 30-minute intervals from Tonzi Ranch span 2001 to May 2022. Variables measured at the flux tower include incoming photosynthetic flux density (PPFD, μmol Photon m^{-2} s^{-1}), vapor pressure deficit (VPD, hPa), air temperature (TA, C), precipitation (PRECIP, mm) and soil moisture at 10, 20 and 30 cm depth, which were averaged to obtain soil water content (SWC,%). Estimates of gross primary productivity (GPP, g C m^{-2} day^{-1}) and ecosystem respiration (RECO, g C m^{-2} day^{-1}) were derived with the eddy covariance method via nighttime partitioning (Baldocchi 2003). Water use efficiency (WUE) is the ratio of carbon gained to water lost via latent heat flux in an ecosystem (GPP/ET). Data were downloaded from the AmeriFlux BASE product, using the principal investigator's gap filling and quality control procedures (GPP_PI_F and RECO_PI_F), which exclude values outside of valid ranges or conditions that fail to meet the turbulent conditions necessary for eddy covariance (Ma et al., 2023). At Tonzi Ranch, gap filling is at a minimum during the dry season, with a maximum of 10 % (in May) and a mean of 6.5 % of gap filled data. Gap filled data correlate well with known measurements; therefore, gap filled data were included in this study.

Bimonthly WTD measurements were collected manually from 2006 to 2022 with a water level meter (Solinst Canada Ltd.). WTD measurements were extended to January 2001 via a modeling approach (Supplemental Material) using reconstructed terrestrial water storage data (Humphrey et al., 2017) and a California Department of Water Resources (DWR) well (number 07N08E36B001M) located 7 km southeast of the site, which provided biannual WTD data 1955 to present, representing the approximate seasonal cycle of minimum and maximum WTD. 30 min WTD measurements were collected with an automatic probe (Global Water Instrument, Model WL 16 U) from 2018 to 2022. Tree ring data from 20 individuals at the site were collected by Cabon et al. (2022) and date back to the mid-1800s (Fig. S3). Together, these long time series enable detection of ecosystem reliance on groundwater for carbon assimilation and allocation to woody growth (Fig. S1).

30 min flux tower data were processed to daily time steps by taking daily averages, except for GPP and RECO, which were summed daily. Bimonthly WTD measurements were linearly interpolated to the daily scale. To minimize the confounding effect of soil moisture, data were subset to the dry season, which was defined as the period between the date of maximum GPP (calculated for each year based on a Tukey smooth curve, typically in May) to October 1. Anomalies were calculated using mean day of year values and then normalized by their standard deviation to obtain z-scores.

We used dendrochronology data to quantify the effect of groundwater on carbon sequestration by building tree ring chronologies using cross-dated measurements from *Quercus douglasii* at the site (Cabon et al., 2022). We detrended series from individual trees with a spline of 50 % frequency cutoff of 30 years, which removed tree size, age, and low-frequency climate signals. At Tonzi ranch, the chronology is 165 years long (dating back to 1856), includes 39 individual series, and has a signal-to-noise ratio of 13.8 (Cabon et al., 2022). To compare this long record with water availability at the site, we used historic estimates spanning 1958-present of PPFD, VPD, TA, and SWC derived from the TerraClimate dataset, which were bilinearly extracted from the pixel over Tonzi (Abatzoglou et al., 2018) (Supplemental Material, Fig. S3). Yearly median growth values for the growing season (Februrary-September) were calculated across all individuals to reduce noise. The tree growth and eddy covariance flux tower data sets represent independent estimates of carbon fluxes at Tonzi ranch over different time scales (daily vs. annual).

The following two sections outline methods to test our hypotheses. First, we calculate daily ecosystem groundwater use from continuous WTD measurements. We then outline three machine learning algorithms to predict GPP, RECO and tree growth anomalies and isolate the effect of groundwater on carbon cycling.

3.2. Diurnal groundwater depletion

Continuous WTD measurements provide insight into daily ecosystem groundwater use. Slopes of WTD drawdown and recharge between diurnal minima and maxima can be used to approximate daily ecosystem groundwater use following the White method (Steven et al., 2005; Butler et al., 2007). Taking the difference between rates of recharge at night and drawdown during the day allows for approximation of ecosystem groundwater usage (Fig. 2). T_g (mm day^{-1}), the daily vegetative groundwater uptake, can be approximated from diurnal fluctuations (Steven et al., 2005):

$$T_g = S_y * \left(\frac{\Delta s_{day}}{t} + R\right)$$

where S_y is the specific yield (estimated for this site to be 0.056, dimensionless) (Miller et al., 2010), Δs_{day} is the difference (mm) between maximum and minimum WTD from 6:00 to 15:00, t is the time (hours) between these time steps, and R is the rate (mm hr^{-1}) of recharge

between 22:00 and 5:00. Recharge is likely driven by snowmelt from the Sierra Nevada (Ma et al., 2016). Fig. 2 shows time series of continuous WTD measurements during the dry season and over the course of a week in June 2020.

The White method relies on the following assumptions: (1) daytime water draw down is the sum of recharge and depletion by the ecosystem, (2) plants are not drawing water from groundwater during the night, (3) the rate of recharge is constant throughout both day and night, and (4) the specific yield can be determined (Loheide II, Butler Jr., and Gorelick 2005). Trees may continue redistributing water from deeper water sources during the night via hydraulic redistribution (Lee et al., 2005). This would result in a depressed recharge rate at nighttime and smaller total T_g. The values of T_g presented herein are potentially an underestimate and ecosystem use of groundwater may be even higher than calculated if hydraulic redistribution occurs. The White method has been used previously at Tonzi Ranch by Miller et al. (2010), who showed that atmospheric pressure, nearby water bodies, and anthropogenic pumping have no effect on continuous WTD measurements at the site (Miller et al., 2010).

T_g can be used to explore ecosystem reliance on groundwater for both carbon assimilation and transpiration.

3.3. Statistical methods

To isolate the effect of WTD on carbon cycling, three machine learning algorithms of varying complexity were trained to predict GPP, RECO and tree growth anomalies. The algorithms included a random forest (RF), neural network (NN), and generalized additive model (GAM). Using a variety of models provides improved prediction power as well as insight into model structure and variable importance. For each algorithm, two models were trained: one including (FULL) and one without (No-WTD) WTD anomaly data. Both the FULL and No-WTD models included PPFD, SWC, TA and VPD training data. GPP (GPP_r), RECO ($RECO_r$), and growth ($Growth_r$) residuals were calculated by subtracting observed from predicted GPP, RECO and growth anomalies from the No-WTD models. GPP_r, RECO ($RECO_r$), and $Growth_r$ therefore correspond to the isolated effect of WTD on GPP, RECO and tree growth, respectively, with the assumption that no other variables besides PPFD, VPD, SWC, and TA affect carbon cycling. FULL models provide information about the importance of WTD in predicting carbon assimilation, respiration, and sequestration at the site when compared to No-WTD models. Further discussion on GAM and NN model structure and training is provided in the Supplemental Material.

Random forest (RF) algorithms were trained using the *randomForest* package in R, and hyperparameter tuning was accomplished with a grid search with 500, 500 and 50 trees for the GPP, RECO and tree growth datasets, respectively, using the *ranger* package in R to optimize minimum node size and sample size. Trees were trained on a random 80 % sample of data. RF models are less prone to overfitting than other model approaches by using a bootstrap bagging approach (Breiman 2001). Variable importance values for the RFs were determined by their mean positioning within the RF trees, with variables closer to initial nodes receiving higher importance.

4. Results and discussion

4.1. WTD and SWC decoupling

Given the lack of precipitation in the summer months, WTD variability exceeds SWC variability in the dry season. Soil moisture and groundwater have different temporal and seasonal dynamics, with soil moisture beginning to decline in late April, before WTD reaches its peak in early June (Figs. S1 and S2). Daily soil moisture and WTD anomalies are largely decoupled during the dry season ($R^2 = 0.14$) when precipitation is rare, maintaining dry surface conditions, while lateral flow from melting snow pack in the Sierra Nevada replenishes groundwater (Baldocchi et al., 2021; Ma et al., 2016). Fig. 1 shows the extent of decoupling between WTD and SWC anomalies each year during the dry season. SWC anomalies often plateau near 0 (reaching average conditions) in the late summer as the shallow soil column desiccates, while WTD anomalies often remain larger in magnitude throughout the dry season. For example, in 2017, WTD anomalies were positive, while SWC anomalies remained near 0, suggesting dry to normal soil water conditions but wetter-than-average groundwater conditions. This pattern is also visible in Figure S2, which shows that WTD has much greater variability during the summer than SWC. While SWC and WTD sometimes contain overlapping information, WTD also has distinct dynamics that may uniquely affect carbon cycling, especially under soil moisture drought.

4.2. Daily WTD use

Continuous WTD data at the site reveal the ecosystem uses more groundwater during periods of greater carbon assimilation and evapotranspiration (Fig. 3). Linear regressions between daily GPP, ET, and WUE all show significant relationships ($p<0.01$) with daily vegetative groundwater uptake (T_g) during the dry season. As these data are derived from a variety of soil moisture conditions, the explanatory power of T_g on GPP, ET and WUE is only moderate, with R^2 values of 0.182, 0.211, and 0.061, respectively. Generally, larger T_g is generally associated with higher ET and GPP, shallower WTD, and lower WUE. Alternatively, smaller T_g corresponds to diminished ET and GPP, deeper WTD and higher WUE. Differences of GPP, ET and WUE are greater between extreme T_g percentiles (0–10 and 90–100 %, representing low and high groundwater use, respectively), all of which demonstrate significant differences ($p<0.01$) using a Student's unpaired *t*-test (Table 1). GPP increases by 6.79 ± 0.97 g C m^{-2} day^{-1} and by 11.96 ± 0.72 g C m^{-2} day^{-1} between extreme low and high T_g and WTD percentiles, respectively. ET rates show a similar increase under high WTD and T_g, and WUE decreases under high T_g and WTD. Higher rates of groundwater use correspond to a less conservative water use strategy, in which WUE is decreased and the system fixes more carbon.

Low values of T_g under dry WTD conditions suggests diminished use of groundwater below a threshold of approximately ~–8 m, the mean WTD over the course of the 20-year time series, corresponding to depressed GPP (Fig. 2). This suggests that mean maximum rooting depth at Tonzi may be shallower than –8 m, below which individuals have difficulty accessing groundwater. Although oaks in California have been shown to grow roots up to 21 m deep to reach groundwater, there is significant spatial heterogeneity, with rooting depth following the capillary fringe just above the water table to avoid anoxic conditions (Lewis and Burgy 1964). WUE represents plant strategy to conserve water while continuing to fix carbon during periods of water stress and is related both VPD and SWC (Peters et al., 2018). The oaks are well-adapted to extreme drought and can withstand large negative water potential gradients of –6.8 MPa and are able to closely regulate transpiration and WUE (Xu and Baldocchi 2003; Chen et al., 2008). Oaks opportunistically use groundwater depending on its availability, drawing down groundwater more quickly when it is plentiful and conserving water during groundwater drought to reach similar fall WTD levels regardless of spring WTD (Baldocchi et al., 2021), or when WTD falls out of reach (Fig. 2).

The site exhibits spatially heterogeneous soil depth and bedrock structure (Raz-Yaseef et al., 2013), and one WTD probe may not be representative of absolute WTD for the entire site. However, the continuous probe WTD levels correlate well ($R^2 = 0.97$, data not shown) with two other wells nearby within the flux tower footprint, suggesting the well is representative of mean relative WTD depth across the ecosystem.

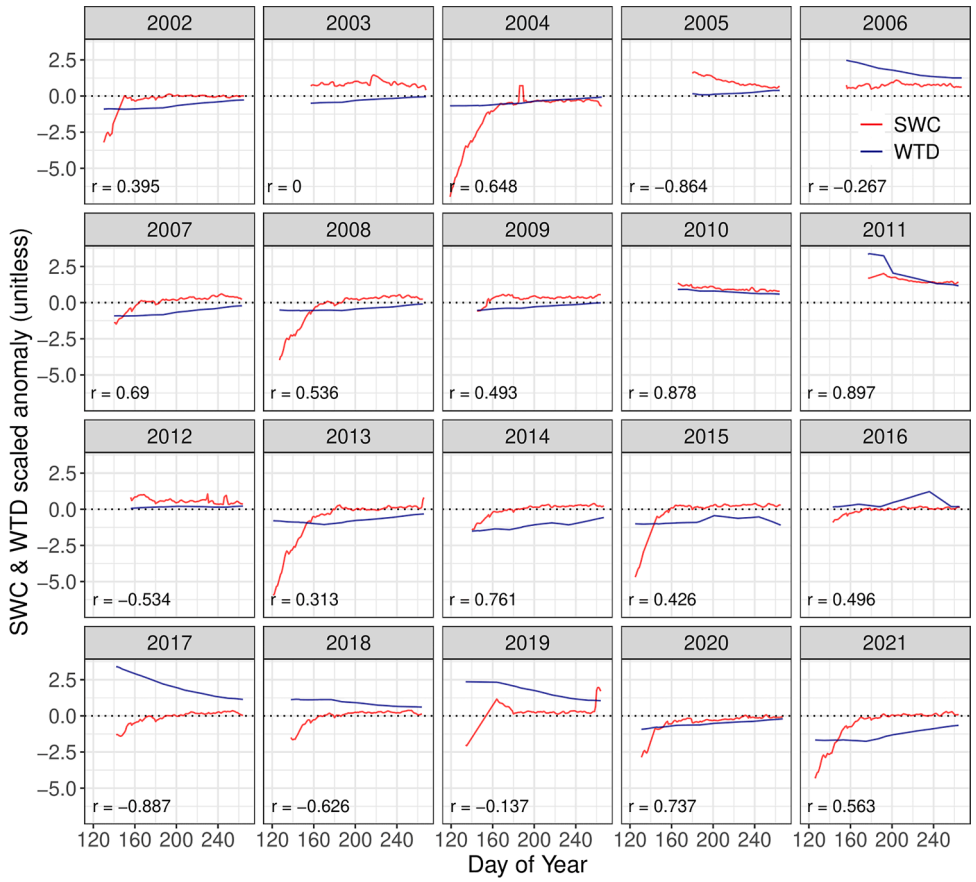

Fig. 1. Dry season water table depth (WTD, blue) and soil water content (SWC, red) scaled Z-score day-of-year anomalies (unitless) by year, 2002–2021. Gray dotted lines at $y = 0$ represent mean conditions for each day of year. r values denote correlation coefficients between WTD and SWC for each year.

Table 1
Outcome of Student's t-tests between extreme negative (0–10 %) and positive (90–100 %) WTD and T_g percentiles for GPP, ET and WUE. For WTD, these correspond to red and blue boxes in Fig. 3, and for T_g, dark blue and green. 0–10 % and 90–100 % are mean values of GPP, ET and WUE under extreme negative and positive WTD and T_g anomalies, respectively. **Δ** is the difference in means between extreme WTD and T_g percentiles. For T_g, **Δ** represents the change in GPP, ET, and WUE between low and high groundwater use. For WTD, **Δ** represents the change in GPP, ET, and WUE between periods of dry and wet groundwater conditions.

	Variable	T-value	P-value	0–10 %	90–100 %	Δ
T_g	GPP	6.99	<0.001	5.31	12.10	6.79 ± 0.97
	ET	6.78	<0.001	0.28	0.95	0.67 ± 0.10
	WUE	–2.82	0.006	21.87	16.20	–5.67 ± 2.01
WTD	GPP	16.66	<0.001	3.54	15.49	11.96 ± 0.72
	ET	14.50	<0.001	0.19	1.40	1.21 ± 0.08
	WUE	–6.73	<0.001	26.50	12.29	–14.22 ± 2.11

4.3. Model performance

GPP, RECO, and tree growth anomaly predictions improved when WTD was included (FULL models) for the RF algorithm (Fig. 4, Table 2). R^2 increased from 0.70 to 0.79, with a decrease in root mean squared error (RMSE) of 0.089 (from 0.56 to 0.47) between the No-WTD and FULL models, respectively, for GPP. Similarly, R^2 increased from 0.72 to 0.79, with a decrease in RMSE of 0.07 (from 0.55 to 0.48) between the No-WTD and FULL models, respectively, for RECO. Linear regression slopes between predicted and observed GPP and RECO remained relatively unchanged between FULL and No-WTD algorithms. For tree growth, R^2 increased from 0.72 to 0.80, with an improvement in slope from 1.55 to 1.41 and decrease in RMSE of 0.07 (from 0.44 to 0.37), between the No-WTD and FULL models, respectively. NN and GAM GPP algorithms produced similar results, with increases in R^2, decreases in RMSE, and little change in slope, between No-WTD and FULL models (Fig. S4, Table S1).

WTD emerged as the second-most important variable in predicting GPP and RECO anomalies after SWC in the FULL models, and incorporating WTD led to a decrease in SWC importance from the No-WTD to the FULL models. Similar results were found for GPP in the GAM and NN algorithms (Fig. 9). These findings suggest that, as expected, WTD and SWC are related and contain some overlapping information; however, as model predictive ability significantly increased when WTD was included for GPP and RECO ($p<0.05$), WTD also has a unique effect on carbon cycling at the site.

WTD was the third-most important variable in predicting tree growth anomalies in the FULL model after VPD and PPFD. SWC importance significantly diminished in the FULL models relative to the No-WTD models, suggesting SWC and WTD contain overlapping information (Fig. 4). This large difference may also be due to a small training dataset ($n = 58$ years) or colinearity between input variables like PPFD and VPD. Finally, individual drivers may have diminished effects on tree growth at the annual scale (Cabon et al., 2022). Despite these limitations, the RF algorithm demonstrated significant improvement in predictive ability between No-WTD and FULL models, suggesting that WTD uniquely and significantly affects carbon allocation to woody growth at the site.

Figure S5 shows details of the FULL GAM algorithm smooth terms, a visual representation of the relationships between all training variables and GPP anomalies. Smooth terms are appropriate given expected relationships between GPP and its various drivers. For example, GPP saturates at high PPFD, corresponding to a light saturation response, and

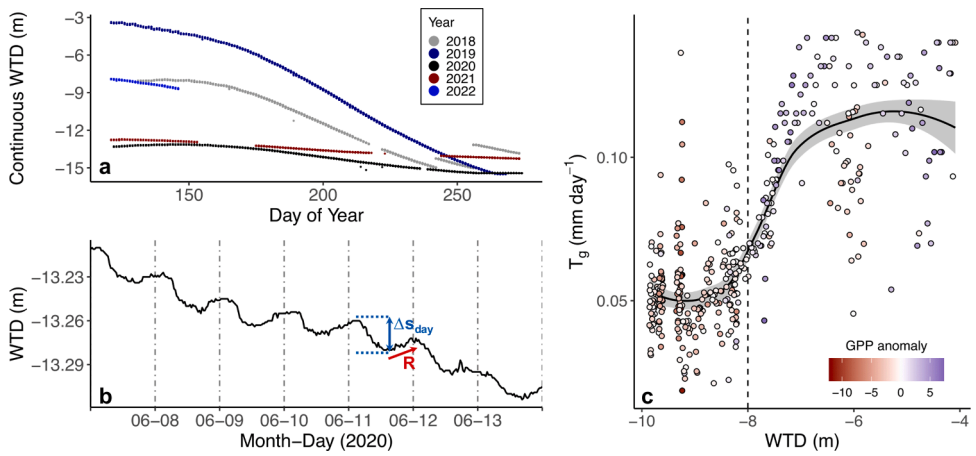

Fig. 2. Continuous water table depth (WTD) levels correspond to groundwater-derived transpiration (T_g). Continuous WTD measurements over a) the dry season by day of year (colors mark years from 2018 to 2022) and b) a week in June 2020 (dotted lines mark midnight), with Δs_{day} and R depicted in blue and red, respectively. c) WTD vs. T_g, colored by gross primary productivity anomalies (GPP) with a loess smooth (solid black line) and standard error (gray shading). Mean WTD over the course of the 20-year time series is –8 m (dashed line), which also corresponds to a threshold below which T_g and GPP anomalies are significantly ($p<0.001$) diminished relative to shallower WTD, suggesting limited access to groundwater.

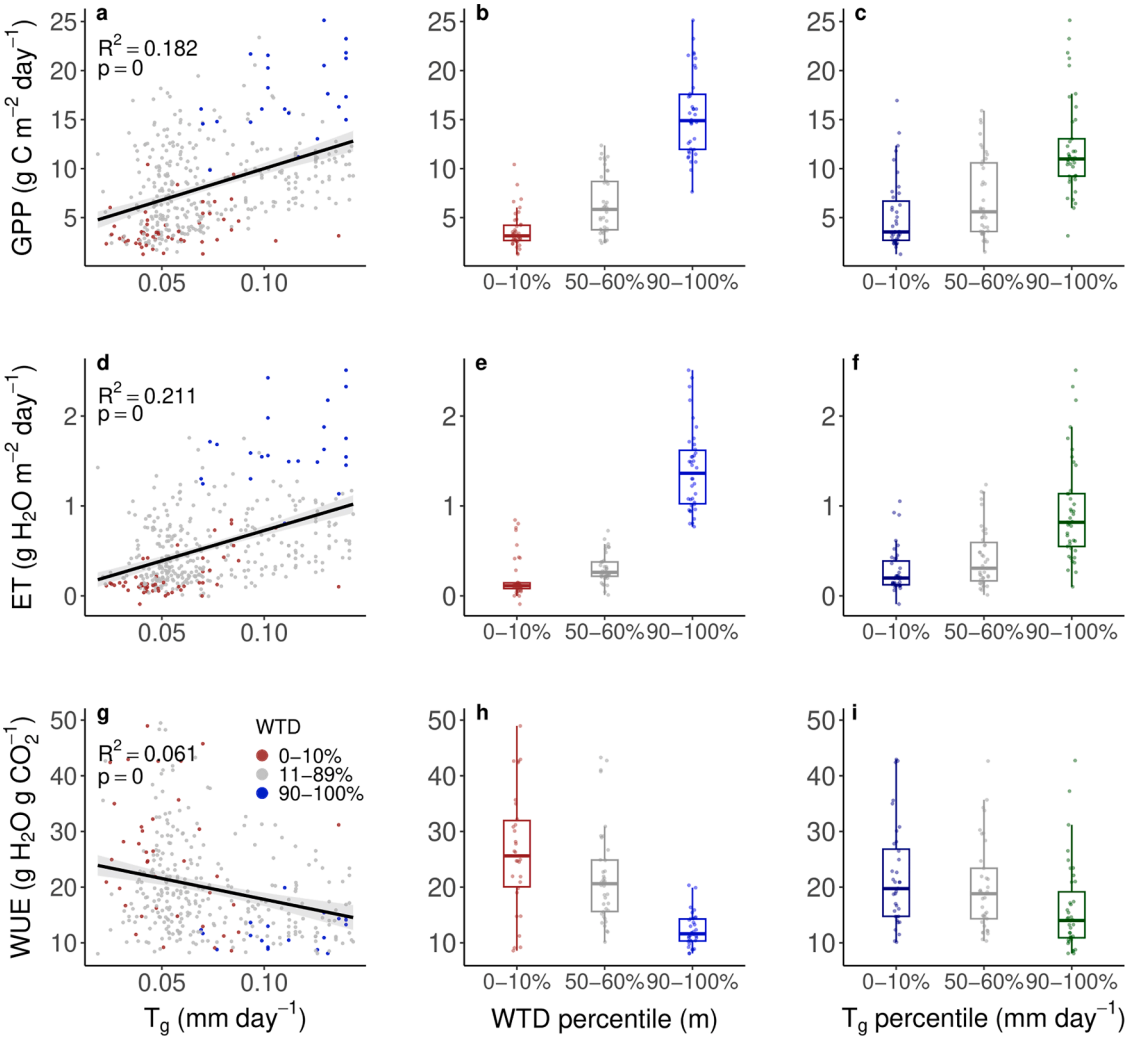

Fig. 3. Continuous WTD measurements reveal ecosystem use of groundwater. a) T_g versus GPP with linear regression and colors representing extreme dry (0–10 %, red), wet (90–100 %, blue) and normal (11–89 %, gray) WTD anomaly percentiles. b) Boxplot of GPP binned by extreme dry (0–10 %, red), average (50–60 %) and extreme wet (90–100 %) WTD percentiles. c) GPP binned by T_g percentiles of low (0–10 %, dark blue), average (50–60 %, gray) and high (90–100 %, green) groundwater use. d and g) Same as a), but for ET and WUE, respectively. e and h) Same as b), but for ET and WUE, respectively. f and i) Same as c), but for ET and WUE, respectively. For box plots, thick lines mark median, boxes represent interquartile range, and whiskers show 5 and 95 percentiles.

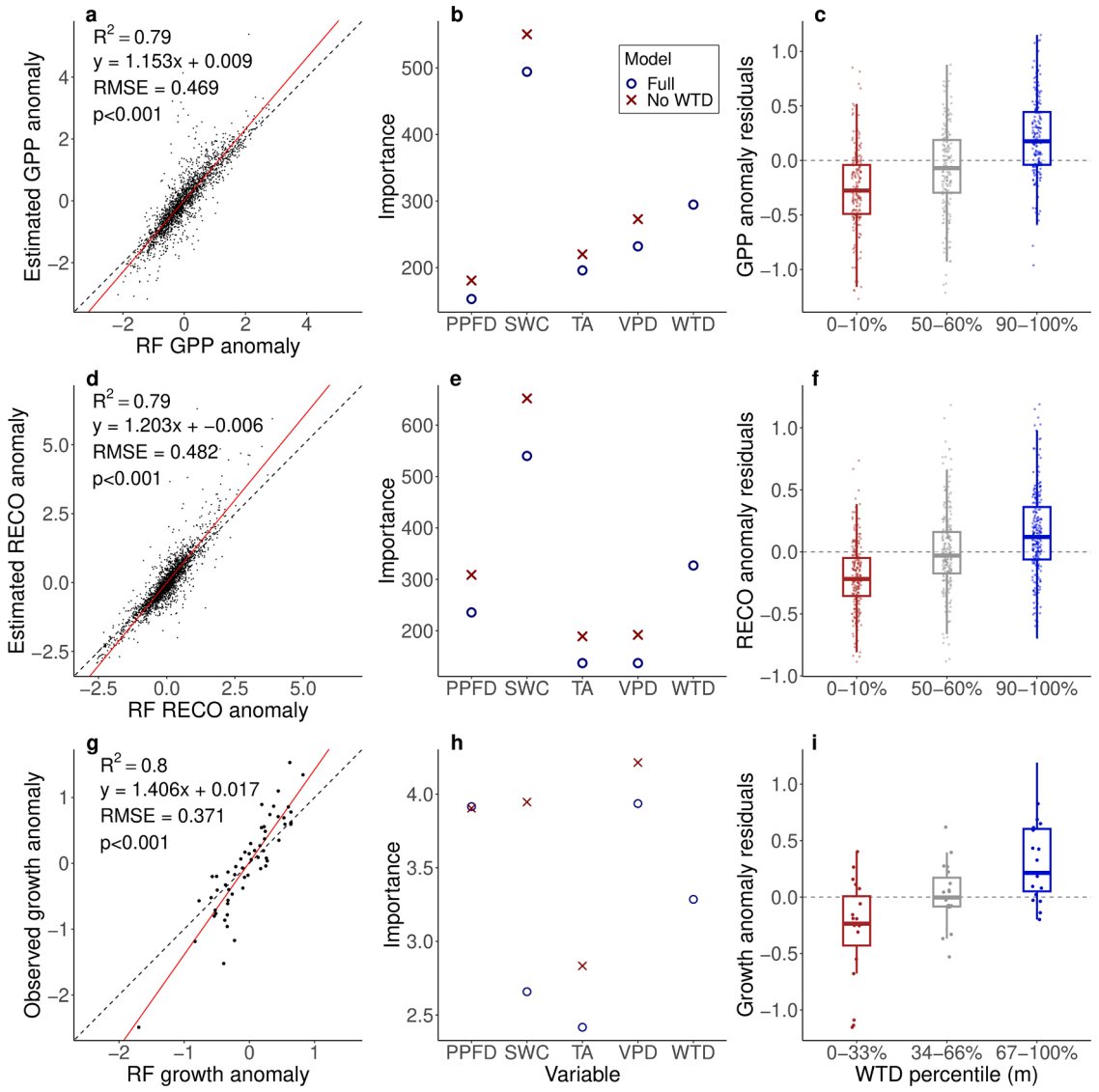

Fig. 4. Random forest predictive skill and importance of WTD for ecosystem function and tree growth. a) Predictions from FULL random forest (RF) model (including WTD) vs. flux tower estimates of canopy GPP (unitless scaled anomaly), with a linear regression (red) equation, R^2, p-value and root mean squared error (RMSE) and 1:1 line (dashed black) for reference. b) Variable importance (unitless) in both FULL (blue) and No-WTD (red) RF models in predicting GPP. c) Residuals from the No-WTD model (GPP_r) binned by 0–10 % (extreme dry/deep WTD, brown), 50–60 % (normal WTD, gray) and 90–100 % (extreme wet/shallow WTD, green) percentiles (m). d-f) Same as a-c, but for RECO. g-i) Same as a-c, but for tree growth. For box plots, thick lines mark median, boxes represent interquartile range, and whiskers show 5 and 95 percentiles.

Table 2
Model predictive performance with (FULL) and without (No-WTD) WTD included in training data of random forest (RF) for flux tower RECO and estimated GPP and tree growth. Models are evaluated via a linear regression between model predictions of and observed daily RECO and GPP and annual median tree growth anomalies. For all models, $p<0.001$.

Variable	Model	Intercept	Slope	RMSE	R^2
GPP	FULL	0.009	1.153	0.47	0.79
	No-WTD	−0.014	1.156	0.56	0.70
RECO	FULL	−0.006	1.203	0.48	0.79
	No-WTD	−0.004	1.202	0.55	0.72
Growth	FULL	0.002	1.406	0.37	0.80
	No-WTD	0.08	1.55	0.44	0.72

high TA and VPD correspond to depressed GPP, as expected under stressful conditions (Farquhar et al., 1980). These smooth terms suggest that the model correctly identifies physiological relationships and increases confidence in its output. WTD and SWC smooth terms have similar shapes, with GPP anomalies increasing with increasing WTD and SWC, and a saturating effect at high positive anomalies. Extreme positive WTD and SWC anomalies led to a slight decrease in GPP, potentially indicating saturated anoxic root conditions that limit carbon assimilation (Skelton et al., 2021).

4.4. WTD dependency

With the assumption that no other variables drive carbon cycling at the site besides VPD, PPFD, SWC, TA and WTD, GPP_r, $RECO_r$ and $Growth_r$ represent isolated relationships between GPP, RECO, tree growth and WTD. Fig. 4 (rightmost column) shows GPP_r, $RECO_r$ and $Growth_r$ versus negative, median, and positive WTD anomalies. For all variables, No-WTD RF model residuals suggest that WTD drought significantly reduces carbon assimilation, respiration and allocation to woody growth at Tonzi Ranch.

GPP_r is significantly ($p < 0.001$) reduced under extreme negative WTD anomalies (0–10 percentiles, $WTD_{0-10\%}$) compared to extreme

positive WTD anomalies (90–100 percentiles, $WTD_{90-100\%}$). Similarly, extreme negative WTD anomalies result in significant reductions in RECO compared to positive WTD anomalies ($p < 0.001$). Finally, tree growth is significantly reduced for negative WTD ($WTD_{0-33\%}$) compared to positive WTD ($WTD_{67-100\%}$) anomalies. For NN and GAM algorithms, groundwater drought also results in decreased GPP, and wet groundwater conditions result in increased GPP (Figure S4). RECO and tree growth exhibit similar patterns in NN and GAM models (data not shown).

Table 3 shows the outcomes of unpaired Student's t-tests of GPP_r, $RECO_r$ and $Growth_r$ rescaled from Z-score anomalies to physical values, grouped by positive and negative WTD anomaly bins for each No-WTD RF model. A significant ($p<0.01$) increase between negative and positive WTD bins is observed for all variables. In Table 3, Δ_r represents the increase in GPP, RECO (g C m^{-2} day^{-1}) and growth (mm yr^{-1}) between negative and positive WTD anomalies. RF models predict an increase of 1.4 g C m^{-2} day^{-1}, 0.69 g C m^{-2} day^{-1}, and 2.56 mm yr^{-1} for GPP, RECO and tree growth, respectively, under wet WTD relative to drought conditions. Summed over the course of the dry season (May-September), this represents a 19.9 % increase (+210.3 ± 19.4) in total annual GPP (mean annual GPP = 1056 ± 145). Oak savanna systems comprise 45,000 km^2 in California; scaling our results over this area, wet groundwater conditions would result in GPP enhancement of 3.8 PgC (1.8 ppm) per century compared to dry conditions. NN and GAM models suggest an even larger GPP enhancement of 319.05 and 384.6 g C m^{-2} yr^{-1}, respectively.

GPP is a proxy of ecosystem carbon assimilation but does not represent carbon sequestration through increases in soil carbon and biomass. Ecosystems release a large fraction (40–45 %) of fixed carbon via autotrophic and heterotrophic respiration back to the atmosphere after assimilation (Van Oijen et al., 2010). Residuals from the RF models suggest RECO also increases under positive relative to negative WTD anomalies, which is to be expected given increased carbon assimilation rates. However, RECO increases to a lesser degree than GPP (1.4 ± 0.13 vs. 0.69 ± 0.08 for GPP and RECO, respectively, or l50 % of GPP_r). As RECO measurements represent the sum of canopy and understory respiration, this difference may suggest a more limited effect of groundwater on soil respiration. Scaling the difference in GPP and RECO over the dry season, Tonzi Ranch acts as a net sink of 106.5 ± 31.5 (g C m^{-2}) under wet WTD conditions compared to dry conditions, or 10.1 % increase in the net annual carbon sink.

Tree rings measure rates of carbon storage in woody growth, a long-lived carbon pool (Cabon et al., 2022). Results from the tree growth analysis suggest that WTD independently affects tree growth after accounting for the effects of other environmental variables. In the RF model, wet groundwater conditions increased growth by 0.176 ± 0.04 mm per year, or 17.7 % of mean annual growth, relative to dry groundwater conditions. The divergence between net carbon sink (+10.1 %) and tree growth (+17.7 %) rates under wet WTD conditions relative to drought may be the result of differences in data coverage. Instead of being isolated to the dry season, tree ring data is integrated over the full calendar year. Therefore, the increase in growth under wet groundwater conditions suggests groundwater affects carbon allocation to woody growth year-round, with increased allocation to above ground biomass under greater groundwater availability. This divergence may also stem from a gradual shift in ecosystem function, with more recent years experiencing diminished effects of groundwater (potentially due to long-term declines in WTD from reduced snowpack or increased rooting depth allowing continuous access to groundwater even under drought).

Table 3
Outcome of Student's t-tests for GPP, RECO and tree growth rescaled residuals from RF models between positive and negative WTD anomalies. − WTD and + WTD are mean values of daily GPP_r and $RECO_r$ (g C m^{-2} day^{-1}) under extreme negative and positive WTD anomalies (0 – 10% and 90 – 100%), respectively, and mean values of annual median $Growth_r$ (mm yr^{-1}) under negative and positive WTD anomalies, respectively (0 – 33% and 64 – 100%). Δ_r is the difference in means between extreme WTD anomalies, representing declines under dry groundwater conditions with standard error.

Variable	T-value	P-value	− WTD	+ WTD	Δ_r
$GPPT_r$	10.86	<0.001	–1.34	0.07	–1.40 ± 0.13
$RECO_r$	8.29	<0.001	–0.78	–0.082	–0.69 ± 0.08
$Growth_r$	4.98	<0.001	0.91	1.09	–0.176 ± 0.04

Additional analysis comparing on GPP_r and $RECO_r$ from the RF model to unscaled WTD and SWC measurements reveals that WTD has the largest effect on GPP_r and $RECO_r$ during June, July, and August (Fig. 5). These months correspond to the hottest, driest, most stressful conditions at the site. Independent relationships between GPP_r, $RECO_r$ and WTD are most prominent when SWC becomes depleted during the dry season. When SWC variability is low, WTD plays a more prominent and significant role (Table S2), potentially due to a reduction in cavitation and increase in stomatal aperture under stressful VPD and TA conditions. However, early in the dry season (e.g., May), groundwater and GPP_r and $RECO_r$ become decoupled. This corresponds to wetter soil moisture conditions and suggests that the ecosystem experiences decreased reliance on groundwater during this period, or perhaps uses hydraulic redistribution to replenish soil moisture reserves (Orellana et al., 2012). Alternatively, this decoupling could point to groundwater limitation, when deep tap roots are exposed to anoxic conditions (as suggested by the GAM smooth terms during extreme positive WTD anomalies (Fig. S5)).

The results from the GPP, RECO and tree growth models validate our hypothesis that wet groundwater conditions enhance the net carbon sink and tree growth relative to drought conditions at the site. These findings confirm previous work that showed groundwater maintains GPP during surface soil moisture drought at groundwater-dependent sites with increasing importance throughout the dry season (Goulden and Bales 2019; Chen et al., 2019). Groundwater not only acts as a buffer against drought, allowing ecosystems to survive and continue assimilating carbon during dry surface conditions (Mueller et al., 2005; Baldocchi et al., 2021), but also enhances ecosystem productivity in periods of excess (Koirala et al., 2014). In a system that is highly adapted to drought (Baldocchi et al., 2021), oaks at Tonzi employ an opportunistic strategy in which groundwater is used to enhance productivity and growth under wet conditions and sustain the ecosystem during surface drought conditions.

Other conditions at the site also influence carbon cycling, including the fraction of absorbed photosynthetically active radiation (fPAR), a measurement of canopy cover and density. fPAR varies seasonally depending on water conditions at the site, with drought deciduousness decreasing total leaf area (Osuna et al., 2015). fPAR anomalies are not highly correlated with WTD anomalies at Tonzi Ranch during the dry season (R^2 <0.02). fPAR does not vary over the course of the day, unlike WTD, which demonstrates diurnal cycles significantly correlated to GPP, ET and WUE (Section 4.1). To avoid over fitting, we did not include fPAR in training datasets. This choice was shown to have little effect on results, as fPAR was not significantly correlated to GPP residuals from any algorithm, suggesting that its effect on GPP anomalies is minimal during the dry season or is captured by other variables. However, future work should consider the effects of canopy density as well.

5. Conclusion

Carbon assimilation, respiration and allocation to woody growth at Tonzi Ranch are sensitive to groundwater conditions during the dry season. Continuous WTD data show that, relative to negative anomalies, positive WTD anomalies correspond to increased groundwater use, ET, GPP, and decreased water use efficiency. Predictive ability of tree growth and dry season GPP and RECO is significantly improved by incorporating WTD measurements in machine learning algorithms.

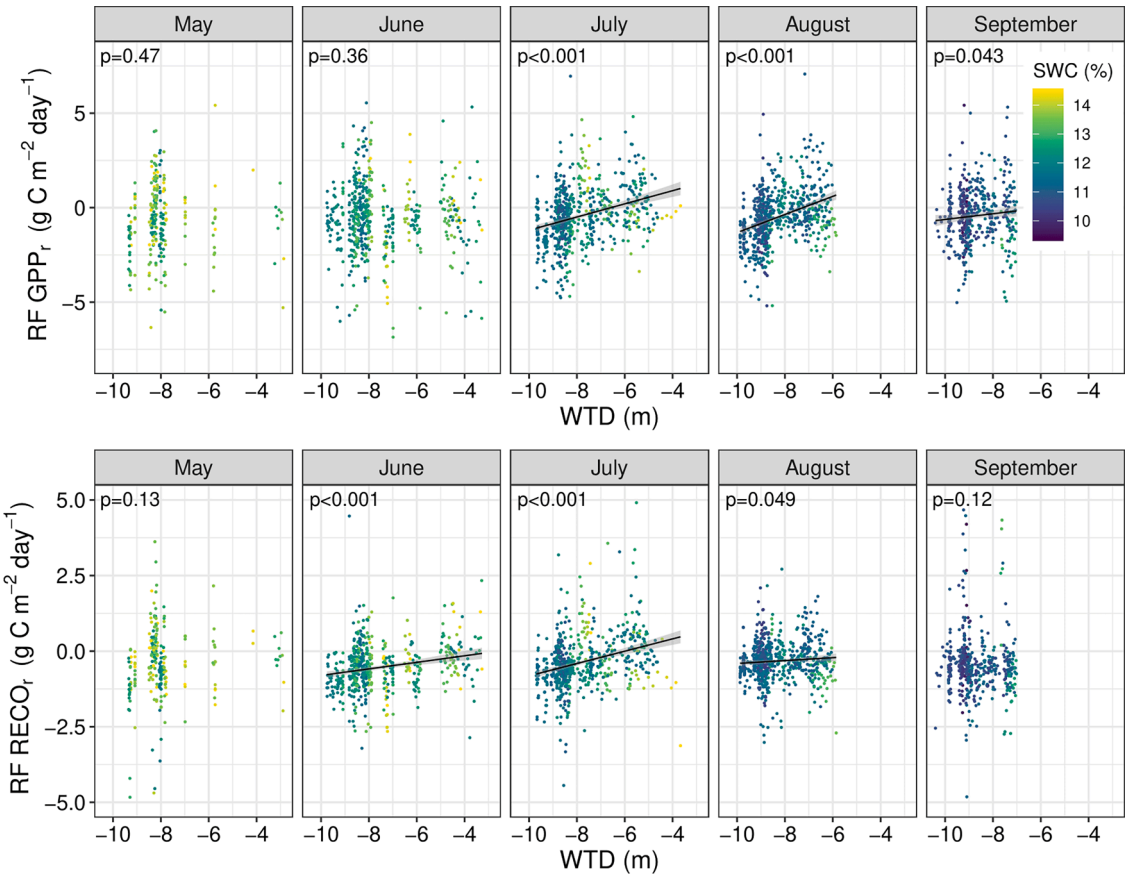

Fig. 5. Effect of groundwater on carbon cycling by month. Water table depth (m) versus residuals from the GPP (GPP_r) and RECO ($RECO_r$) No-WTD RF models (top and bottom rows, respectively) by month (panels) and soil water content (SWC (%), colors). P-values in top left corners are for linear regressions (black) with standard error (gray shading).

Extreme negative WTD anomalies correspond with significant decreases in GPP, RECO and growth, suggesting that groundwater drought diminishes carbon assimilation and respiration, while wet groundwater conditions enhance GPP, RECO and tree growth. Over the course of the dry season, wet groundwater conditions increase carbon assimilation by 210.3 ± 19.4 g C m^{-2}, or 17.7 % of annual GPP. Relative to extreme drought conditions, positive WTD anomalies correspond to a 19.9 % increase in annual tree growth. WTD and SWC contain overlapping information but have unique effects on GPP, RECO, and tree growth, as dry surface conditions can become decoupled from deeper groundwater availability during the dry season.

Differences in GPP, RECO and tree growth rates provide additional insight into ecosystem function. A diminished response of RECO to groundwater drought suggests soil (heterotrophic) respiration is less affected by groundwater, as expected given the depth to the water table at the site and limited soil moisture during the dry season. Decoupling between GPP_r and WTD during May suggests WTD limitation during the wet season, when the water table may introduce anoxic root conditions. Finally, tree growth demonstrates large increases (19.9 % yr^{-1}) under positive WTD anomalies, suggesting that groundwater may support allocation to woody growth throughout the calendar year. Indeed, oak trees in the region have been shown to grow roots up to 21 m deep, regardless of tree diameter, height, or subspecies (Lewis and Burgy, 1964), and rock moisture is a stronger predictor of oak evapotranspiration than soil moisture at a similar blue oak site (Hahm et al., 2022).

The majority of field campaigns at the site and throughout the region have been limited in scope, focusing on one or two growing seasons. Furthermore, the majority of terrestrial biosphere models do not include groundwater-vegetation interactions and lack complex subsurface parameterization (Maxwell and Condon, 2016; Fisher et al., 2014). These omissions make it difficult to quantify groundwater-vegetation feedbacks and identify regions where groundwater-vegetation dynamics are most tightly coupled. Our results show that deep subsurface water availability is an important resource in semi-arid and seasonally-dry phreatophytic ecosystems. Therefore, incorporating physiological relationships between GPP, biomass accumulation, and groundwater may improve carbon cycle modeling and projections.

Groundwater deficits are increasing throughout California (Margulis et al., 2016; Mote et al., 2018). Since 1930, dates of peak snowpack have been becoming earlier at a rate of 0.6 days per decade, resulting in diminished summer snowpacks (Kapnick and Hall, 2010). These 100 km-distant snowpacks recharge groundwater at Tonzi (Ma et al., 2016). Increased human consumption is further diminishing groundwater resources in California and globally (Dettinger et al., 2015; Meixner et al., 2016). Intensifying groundwater drought may decrease carbon assimilation and long term woody biomass accumulation at Tonzi and similar systems, resulting in a positive feedback to climate change. Access to groundwater, however, also may enhance ecosystem resilience under extreme drought (Brodrick and Asner 2017). Mediterranean oak savannas are well-adapted to dry climates, closely regulating their water use strategies based on water resource availability.

At Tonzi Ranch, a core AmeriFlux site, the combination of eddy covariance flux towers and long-term ancillary data sets, such as groundwater measurements and tree growth, enables detection of subtle ecosystem dynamics that would otherwise be challenging to quantify. Therefore, this study also documents the importance of long-term ancillary data, which provide critical contextual information to flux measurements and enable broader understanding of ecosystem function.

Declaration of Competing Interest

The authors declare that they have no known competing financial interests or personal relationships that could have appeared to influence the work reported in this paper.

Data availability

Tonzi Ranch eddy covariance flux tower and groundwater datasets are available through the AmeriFlux server at https://ameriflux.lbl.gov/doi/AmeriFlux/US-Ton/. Dendrochronology data are available at https://datadryad.org/stash/dataset/doi:10.5061/dryad.15dv41nzt. Additional groundwater data spanning 2000-2022 from a Calfironia Department of Water Resources well (#07N08E36B001M) are available at https://wdl.water.ca.gov/. Reconstructed terrestrial water storage time series are available at http://doi.org/10.5905/ethz-1007-85. TerraClimate historic monthly climate and climatic water balance data are available at https://doi.org/10.7923/G43J3B0R.

Acknowledgments

S.R. acknowledges support from NASA FINESST fellowship No. 80NSSC22K1448, the Achievement Rewards for College Scientists (ARCS) fellowship, and the Carol Baird Fieldwork Grant. T.F.K., S.R. and M.G. acknowledge support from a NASA SMAP Award 80NSSC20K1801, and T.F.K. acknowledges support from a DOE Early Career Research Program award #DE-SC0021023. A.C. acknowledges support from the Swiss National Science Foundation through grant number TMPFP3_209811. Funding for data collection at Tonzi Ranch was provided by the U.S. Department of Energy's Office of Science through the AmeriFlux project.

Supplementary materials

Supplementary material associated with this article can be found, in the online version, at doi:10.1016/j.agrformet.2023.109725.

References

Abatzoglou, J.T., Dobrowski, S.Z., Parks, S.A., Hegewisch, K.C., 2018. TerraClimate, a high-resolution global dataset of monthly climate and climatic water balance from 1958 to 2015. Sci. Data 5 (1), 170191. https://doi.org/10.1038/sdata.2017.191.

Ahlström, A., Raupach, M.R., Schurgers, G., Smith, B., Arneth, A., Jung, M., Reichstein, M., et al., 2015. The dominant role of semi-arid ecosystems in the trend and variability of the land CO_2 sink. Science 348 (6237), 895–899. https://doi.org/10.1126/science.aaa1668.

Anderegg, W.R.L., Schwalm, C., Biondi, F., Camarero, J.J., Koch, G., Litvak, M., Ogle, K., et al., 2015. Pervasive drought legacies in forest ecosystems and their implications for carbon cycle models. Science 349 (6247), 528–532. https://doi.org/10.1126/science.aab1833.

Anderegg, W.R.L., Konings, A.G., Trugman, A.T., Yu, K., Bowling, D.R., Gabbitas, R., Karp, D.S., et al., 2018. Hydraulic diversity of forests regulates ecosystem resilience during drought. Nature 561 (7724), 538–541. https://doi.org/10.1038/s41586-018-0539-7.

Anderegg, W.R.L., Trugman, A.T., Badgley, G., Konings, A.G., Shaw, J., 2020. Divergent forest sensitivity to repeated extreme droughts. Nat. Clim. Change 10 (12), 1091–1095. https://doi.org/10.1038/s41558-020-00919-1.

Baldocchi, D.D., 2003. Assessing the eddy covariance technique for evaluating carbon dioxide exchange rates of ecosystems: past, present and future. Glob. Change Biol. 9 (4), 479–492. https://doi.org/10.1046/j.1365-2486.2003.00629.x.

Baldocchi, D., Ma, S., Verfaillie, J., 2021. On the inter- and intra-annual variability of ecosystem evapotranspiration and water use efficiency of an Oak Savanna and annual grassland subjected to booms and busts in Rainfall. Glob. Change Biol. 27 (2), 359–375. https://doi.org/10.1111/gcb.15414.

Breiman, L., 2001. Random forests. Mach. Learn. 45 (1), 5–32. https://doi.org/10.1023/A:1010933404324.

Brodrick, P.G., Asner, G.P., 2017. Remotely sensed predictors of conifer tree mortality during severe drought. Environ. Res. Lett. 12 (11), 115013 https://doi.org/10.1088/1748-9326/aa8f55.

Burgess, S.S.O., Adams, M.A., Turner, N.C., Ong, C.K., 1998. The redistribution of soil water by tree root systems. Oecologia 115 (3), 306–311. https://doi.org/10.1007/s004420050521.

Butler, J.J., Kluitenberg, G.J., Whittemore, D.O., Loheide, S.P., Jin, W., Billinger, M.A., Zhan, X., 2007. A field investigation of phreatophyte-induced fluctuations in the water table: phreatophyte-induced fluctuations. Water Resour. Res. 43 (2) https://doi.org/10.1029/2005WR004627.

Cabon, A., Kannenberg, S.A., Arain, A., Babst, F., Baldocchi, D., Belmecheri, S., Delpierre, N., et al., 2022. Cross-biome synthesis of source versus sink limits to tree growth. Science 376 (6594), 758–761. https://doi.org/10.1126/science.abm4875.

Canadell, J., Jackson, R.B., Ehleringer, J.B., Mooney, H.A., Sala, O.E., Schulze, E.D., 1996. Maximum rooting depth of vegetation types at the global scale. Oecologia 108 (4), 583–595. https://doi.org/10.1007/BF00329030.

Chen, B., Chen, J.M., Baldocchi, D.D., Liu, Y., Wang, S., Zheng, T., Black, T.A., Croft, H., 2019. Including soil water stress in process-based ecosystem models by scaling down maximum carboxylation rate using accumulated soil water deficit. Agric. For. Meteorol. 276-277 (October), 107649 https://doi.org/10.1016/j.agrformet.2019.107649.

Chen, X., Rubin, Y., Ma, S., Baldocchi, D., 2008. Observations and stochastic modeling of soil moisture control on evapotranspiration in a Californian Oak Savanna. Water Resour. Res. 44 (8) https://doi.org/10.1029/2007WR006646.

Chitra-Tarak, R., Xu, C., Aguilar, S., Anderson-Teixeira, K.J., Chambers, J., Detto, M., Faybishenko, B., et al., 2021. Hydraulically-vulnerable trees survive on deep-water access during droughts in a tropical forest. New Phytologist. 231 (5), 1798–1813. https://doi.org/10.1111/nph.17464.

Dawson, T.E., Hahm, W.J., Crutchfield-Peters, K., 2020. Digging deeper: what the critical zone perspective adds to the study of plant ecophysiology. New Phytologist. 226 (3), 666–671. https://doi.org/10.1111/nph.16410.

Dettinger, M., Udall, B., Georgakakos, A., 2015. Western water and climate change. Ecol. Appl. 25 (8), 2069–2093. https://doi.org/10.1890/15-0938.1.

Draper, C.S., Reichle, R.H., Koster, R.D., 2018. Assessment of MERRA-2 land surface energy flux estimates. J. Clim. 31 (2), 671–691. https://doi.org/10.1175/JCLI-D-17-0121.1.

Fan, Y., Miguez-Macho, G., Jobbagy, E.G., Jackson, R.B., Otero-Casal, C., 2017. Hydrologic regulation of plant rooting depth. Proc. Natl. Acad. Sci. 114 (40), 10572–10577. https://doi.org/10.1073/pnas.1712381114.

Fang, Y., Michalak, A.M., Schwalm, C.R., Huntzinger, D.N., Berry, J.A., Ciais, P., Piao, S., et al., 2017. Global land carbon sink response to temperature and precipitation varies with ENSO phase. Environ. Res. Lett. 12 (6), 064007 https://doi.org/10.1088/1748-9326/aa6e8e.

Farquhar, G.D., von Caemmerer, S., Berry, J.A., 1980. A biochemical model of photosynthetic CO_2 assimilation in leaves of C3 species. Planta 149 (1), 78–90. https://doi.org/10.1007/BF00386231.

Fisher, J.B., Huntzinger, D.N., Schwalm, C.R., Sitch, S., 2014. Modeling the terrestrial biosphere. Annu. Rev. Environ. Resour. 39 (1), 91–123. https://doi.org/10.1146/annurev-environ-012913-093456.

Gelaro, R., McCarty, W., Suarez, M.J., Todling, R., Molod, A., Takacs, L., Randles, C.A., et al., 2017. The modern-era retrospective analysis for research and applications, version 2 (MERRA-2). J. Clim. 30 (14), 5419–5454. https://doi.org/10.1175/JCLI-D-16-0758.1.

Geruo, A., Velicogna, I., Zhao, M., Colliander, A., Kimball, J.S., 2020. Satellite detection of varying seasonal water supply restrictions on grassland productivity in the Missouri Basin, USA. Remote Sens. Environ. 239 (March), 111623 https://doi.org/10.1016/j.rse.2019.111623.

Geruoa, A., Velicogna, I., Kimball, J.S., Kim, Y., 2015. Impact of changes in GRACE derived terrestrial water storage on vegetation growth in Eurasia. Environ. Res. Lett. 10 (12), 124024 https://doi.org/10.1088/1748-9326/10/12/124024.

Goulden, M.L., Bales, R.C., 2019. California forest die-off linked to multi-year deep soil drying in 2012-2015 drought. Nat. Geosci. 12 (8), 632. https://doi.org/10.1038/s41561-019-0388-5. +.

Green, J.K., Seneviratne, S.I., Berg, A.M., Findell, K.L., Hagemann, S., Lawrence, D.M., Gentine, P., 2019. Large influence of soil moisture on long-term terrestrial carbon uptake. Nature 565 (7740), 476–479. https://doi.org/10.1038/s41586-018-0848-x.

Hahm, W.J., Dralle, D.N., Sanders, M., Bryk, A.B., Fauria, K.E., Huang, M.H., Hudson-Rasmussen, B., et al., 2022. Bedrock vadose zone storage dynamics under extreme drought: consequences for plant water availability, recharge, and runoff. Water Resour. Res. 58 (4), e2021WR031781 https://doi.org/10.1029/2021WR031781.

Humphrey, V., Gudmundsson, L., Seneviratne, S.I., 2017. A global reconstruction of climate-driven subdecadal water storage variability. Geophys. Res. Lett. 44 (5), 2300–2309. https://doi.org/10.1002/2017GL072564.

Humphrey, V., Zscheischler, J., Ciais, P., Gudmundsson, L., Sitch, S., Seneviratne, S.I., 2018. Sensitivity of atmospheric CO_2 growth rate to observed changes in terrestrial water storage. Nature 560 (7720), 628–631. https://doi.org/10.1038/s41586-018-0424-4.

Jackson, R.B., Canadell, J., Ehleringer, J.R., Mooney, H.A., Sala, O.E., Schulze, E.D., 1996. A global analysis of root distributions for terrestrial biomes. Oecologia 108 (3), 389–411. https://doi.org/10.1007/BF00333714.

Kapnick, S., Hall, A., 2010. Observed climate–snowpack relationships in California and their implications for the future. J. Clim. 23 (13), 3446–3456. https://doi.org/10.1175/2010JCLI2903.1.

Kibler, CL., Schmidt, E.C, Roberts, D.A., Stella, J.C., Kui, L., Lambert, A.M., Singer, M.B., 2021. A brown wave of riparian woodland mortality following groundwater declines during the 2012,Ä¡2019 California Drought. Environ. Res. Lett. 16 (8), 084030 https://doi.org/10.1088/1748-9326/ac1377.

Kirchner, J.W., Godsey, S.E., Solomon, M., Osterhuber, R., McConnell, J.R., Penna, D., 2020. The pulse of a montane ecosystem: coupling between daily cycles in solar flux,

snowmelt, transpiration, groundwater, and Streamflow at Sagehen creek and independence creek, Sierra Nevada, USA. Hydrol. Earth Syst. Sci. 24 (11), 5095–5123. https://doi.org/10.5194/hess-24-5095-2020.
Kleidon, AL., Heimann, M., 1998a. A method of determining rooting depth from a terrestrial biosphere model and its impacts on the global water and carbon cycle. Glob. Change Biol. 4 (3), 275–286. https://doi.org/10.1046/j.1365-2486.1998.00152.x.
Kleidon, A., Heimann, M., 1998b. Optimised rooting depth and its impacts on the simulated climate of an atmospheric general circulation model. Geophys. Res. Lett. 25 (3), 345–348. https://doi.org/10.1029/98GL00034.
Klos, P.Z., Goulden, M.L., Riebe, C.S., Tague, C.L., Toby O'Geen, A., Flinchum, B.A., Safeeq, M., et al., 2018. Subsurface plant-accessible water in mountain ecosystems with a mediterranean climate. WIREs Water 5 (3), e1277. https://doi.org/10.1002/wat2.1277.
Koirala, S., Jung, M., Reichstein, M., Graaf, I.E.M., Camps-Valls, G., Ichii, K., Papale, D., et al., 2017. Global distribution of groundwater-vegetation spatial covariation. Geophys. Res. Lett. 44 (9), 4134–4142. https://doi.org/10.1002/2017GL072885.
Koirala, S., Yeh, P.J.F., Hirabayashi, Y., Kanae, S., Oki, T., 2014. Global-scale land surface hydrologic modeling with the representation of water table dynamics. J. Geophys. Res. Atmos. 119 (1), 75–89. https://doi.org/10.1002/2013JD020398.
Koteen, L.E., Raz-Yaseef, N., Baldocchi, D.D., 2015. Spatial heterogeneity of fine root biomass and soil carbon in a California Oak Savanna illuminates plant functional strategy across periods of high and low resource supply. Ecohydrology 8 (2), 294–308. https://doi.org/10.1002/eco.1508.
Lee, J.E., Oliveira, R.S., Dawson, T.E., Fung, I., 2005. Root functioning modifies seasonal climate. Proc. Natl. Acad. Sci. 102 (49), 17576–17581. https://doi.org/10.1073/pnas.0508785102.
Lewis, D.C., Burgy, R.H., 1964. The relationship between oak tree roots and groundwater in fractured rock as determined by tritium tracing. J. Geophys. Res. 69 (12), 2579–2588. https://doi.org/10.1029/JZ069i012p02579 (1896-1977).
Li, W., Migliavacca, M., Forkel, M., Denissen, J.M.C., Reichstein, M., Yang, H., Duveiller, G., Weber, U., Orth, R., 2022. Widespread increasing vegetation sensitivity to soil moisture. Nat. Commun. 13 (1), 3959. https://doi.org/10.1038/s41467-022-31667-9.
Liu, Y., Konings, A.G., Kennedy, D., Gentine, P., 2021. Global coordination in plant physiological and rooting strategies in response to water stress. Glob. Biogeochem. Cycles 35 (7). https://doi.org/10.1029/2020GB006758 e2020GB006758.
Loheide II, Steven, P., Butler Jr., J.J., Gorelick, S.M., 2005. Estimation of groundwater consumption by phreatophytes using diurnal water table fluctuations: a saturated-unsaturated flow assessment. Water Resour. Res. 41 (7) https://doi.org/10.1029/2005WR003942.
Ma, S., Baldocchi, D., Wolf, S., Verfaillie, J., 2016. Slow ecosystem responses conditionally regulate annual carbon balance over 15 years in Californian Oak-Grass Savanna. Agric. For. Meteorol. 228-229 (November), 252–264. https://doi.org/10.1016/j.agrformet.2016.07.016.
Ma, S., Xu, L., Verfaillie, J., Baldocchi, D., 2023. AmeriFlux BASE US-Ton Tonzi Ranch, Ver. AmeriFlux AMP, p. 17. https://doi.org/10.17190/AMF/1245971, 5.
Margulis, S.A., Cortés, G., Girotto, M., Huning, L.S., Li, D., Durand, M., 2016. Characterizing the extreme 2015 snowpack deficit in the Sierra Nevada (USA) and the implications for drought recovery. Geophys. Res. Lett. 43 (12), 6341–6349. https://doi.org/10.1002/2016GL068520.
Maxwell, R.M., Condon, L.E., 2016. Connections between groundwater flow and transpiration partitioning. Science 353 (6297), 377–380. https://doi.org/10.1126/science.aaf7891.
Maxwell, R.M., Putti, M., Meyerhoff, S., Delfs, J.O., Ferguson, I.M., Ivanov, V., Kim, J., et al., 2014. Surface-subsurface model intercomparison: a first set of benchmark results to diagnose integrated hydrology and feedbacks. Water Resour. Res. 50 (2), 1531–1549. https://doi.org/10.1002/2013WR013725.
McCormick, E.L., Dralle, D.N., Jesse Hahm, W., Tune, A.K., Schmidt, L.M., Dana Chadwick, K., Rempe, D.M., 2021. Widespread woody plant use of water stored in bedrock. Nature 597 (7875), 225–229. https://doi.org/10.1038/s41586-021-03761-3.
McElrone, A.J., Pockman, W.T., Martinez-Vilalta, J., Jackson, RB., 2004. Variation in xylem structure and function in stems and roots of trees to 20m depth. New Phytologist. 163 (3), 507. https://doi.org/10.1111/j.1469-8137.2004.01127.x, 17.
Meixner, T., Manning, A.H., Stonestrom, D.A., Allen, D.M., Ajami, H., Blasch, K.W., Brookfield, A.E., et al., 2016. Implications of projected climate change for groundwater recharge in the Western United States. J. Hydrol. 534 (March), 124–138. https://doi.org/10.1016/j.jhydrol.2015.12.027 (Amst).
Meyers, Z.P., Frisbee, M.D., Rademacher, L.K., Stewart-Maddox, N.S., 2021. Old groundwater buffers the effects of a major drought in groundwater-dependent ecosystems of the Eastern Sierra Nevada (CA). Environ. Res. Lett. 16 (4), 044044 https://doi.org/10.1088/1748-9326/abde5f.
Miller, G.R., Chen, X., Rubin, Y., Ma, S., Baldocchi, D.D., 2010. Groundwater uptake by woody vegetation in a semiarid Oak Savanna. Water Resour. Res. 46 (10) https://doi.org/10.1029/2009WR008902.
Mote, P.W., Li, S., Lettenmaier, D.P., Xiao, M., Engel, R., 2018. Dramatic declines in snowpack in the Western US. Npj Clim. Atmos. Sci. 1 (1), 1–6. https://doi.org/10.1038/s41612-018-0012-1.
Mu, M., De Kauwe, M.G., Ukkola, A.M., Pitman, A.J., Guo, W., Hobeichi, S., Briggs, P.R., 2021. Exploring how groundwater buffers the influence of heatwaves on vegetation function during multi-year droughts. Earth Syst. Dyn. 12 (3), 919–938. https://doi.org/10.5194/esd-12-919-2021.
Mueller, R.C., Scudder, C.M., Porter, M.E., Talbot Trotter, R., Gehring, C.A., Whitham, T. G., 2005. Differential tree mortality in response to severe drought: evidence for long-term vegetation shifts. J. Ecol. 93 (6), 1085–1093. https://doi.org/10.1111/j.1365-2745.2005.01042.x.
Neumann, R.B., Cardon, Z.G., 2012. The magnitude of hydraulic redistribution by plant roots: a review and synthesis of empirical and modeling studies. New Phytologist. 194 (2), 337–352. https://doi.org/10.1111/j.1469-8137.2012.04088.x.
Orellana, F., Verma, P., Loheide, S.P., Daly, E., 2012. Monitoring and modeling water-vegetation interactions in groundwater-dependent ecosystems. Rev. Geophys. 50 (3) https://doi.org/10.1029/2011RG000383.
Osuna, J.L., Baldocchi, D.D., Kobayashi, H., Dawson, T.E., 2015. Seasonal trends in photosynthesis and electron transport during the mediterranean summer drought in leaves of Deciduous Oaks. Tree Physiol. 35 (5), 485–500. https://doi.org/10.1093/treephys/tpv023.
Peters, W., Velde, I.R., Schaik, E., Miller, J.B., Ciais, P., Duarte, H.F., Laan-Luijkx, I.T., et al., 2018. Increased water-use efficiency and reduced CO_2 uptake by plants during droughts at a continental scale. Nat. Geosci. 11 (10), 744–748. https://doi.org/10.1038/s41561-018-0212-7.
Raz-Yaseef, N., Koteen, L., Baldocchi, D.D., 2013. Coarse root distribution of a semi-arid Oak Savanna estimated with ground penetrating radar. J. Geophys. Res. Biogeosciences 118 (1), 135–147. https://doi.org/10.1029/2012JG002160.
Ridolfi, L., D'Odorico, P., Laio, F., 2006. Effect of vegetation, water table feedbacks on the stability and resilience of plant ecosystems. Water Resour. Res. 42 (1) https://doi.org/10.1029/2005WR004444.
Roebroek, C.T.J., Melsen, L.A., Dijke, A.J.H, Fan, Y., Teuling, A.J., 2020. Global distribution of hydrologic controls on forest growth. Hydrol. Earth Syst. Sci. 24 (9), 4625–4639. https://doi.org/10.5194/hess-24-4625-2020.
Shevliakova, E., Stouffer, R.J., Malyshev, S., Krasting, J.P., Hurtt, G.C., Pacala, S.W., 2013. Historical warming reduced due to enhanced land carbon uptake. Proc. Natl. Acad. Sci. U. S. A. 110 (42), 16730–16735. https://doi.org/10.1073/pnas.1314047110.
Skelton, R.P., Anderegg, L.D.L., Diaz, J., Kling, M.M., Papper, P., Lamarque, L.J., Delzon, S., Dawson, T.E., Ackerly, D.D., 2021. Evolutionary relationships between drought-related traits and climate shape large hydraulic safety margins in Western North American Oaks. Proc. Natl. Acad. Sci. 118 (10) https://doi.org/10.1073/pnas.2008987118.
Stocker, B.D., Tumber-Dávila, S.J., Konings, A.G., Anderson, M.C., Hain, C., Jackson, R. B., 2023. Global patterns of water storage in the rooting zones of vegetation. Nat. Geosci. 1–7. https://doi.org/10.1038/s41561-023-01125-2. February.
Stocker, B.D., Zscheischler, J., Keenan, T.F., Prentice, I.C., Penuelas, J., Seneviratne, S.I., 2018. Quantifying soil moisture impacts on light use efficiency across biomes. New Phytologist. 218 (4), 1430–1449. https://doi.org/10.1111/nph.15123.
Thompson, S.E., Harman, C.J., Konings, A.G., Sivapalan, M., Neal, A., Troch, P.A., 2011. Comparative hydrology across ameriflux sites: the variable roles of climate, vegetation, and groundwater. Water Resour. Res. 47 (10) https://doi.org/10.1029/2010WR009797.
Tumber-Dávila, S., Jochen Schenk, J.H., Du, E., Jackson, R.B., 2022. Plant sizes and shapes above and belowground and their interactions with climate. New Phytologist. 235 (3), 1032–1056. https://doi.org/10.1111/nph.18031.
Van Oijen, M., Schapendonk, A., Höglind, M., 2010. On the relative magnitudes of photosynthesis, respiration, growth and carbon storage in vegetation. Ann. Bot. 105 (5), 793–797. https://doi.org/10.1093/aob/mcq039.
Xu, C., McDowell, N.G., Fisher, R.A., Wei, L., Sevanto, S., Christoffersen, B.O., Weng, E., Middleton, R.S., 2019. Increasing impacts of extreme droughts on vegetation productivity under climate change. Nat. Clim. Change 9 (12), 948–953. https://doi.org/10.1038/s41558-019-0630-6.
Xu, L., Baldocchi, D.D., 2003. Seasonal trends in photosynthetic parameters and stomatal conductance of Blue Oak (Quercus Douglasii) under prolonged summer drought and high temperature. Tree Physiol. 23 (13), 865–877. https://doi.org/10.1093/treephys/23.13.865.
Yan, B., Dickinson, R.E., 2014. Modeling hydraulic redistribution and ecosystem response to droughts over the amazon basin using community land model 4.0 (CLM4). J. Geophys. Res. Biogeosciences 119 (11), 2130–2143. https://doi.org/10.1002/2014JG002694.
Yang, Y., Donohue, R.J., McVicar, T.R., 2016. Global estimation of effective plant rooting depth: implications for hydrological modeling. Water Resour. Res. 52 (10), 8260–8276. https://doi.org/10.1002/2016WR019392.
Zhang, F., Biederman, J.A., Dannenberg, M.P., Yan, D., Reed, S.C., Smith, W.K., 2021. Five decades of observed daily precipitation reveal longer and more variable drought events across much of the Western United States. Geophys. Res. Lett. 48 (7) https://doi.org/10.1029/2020GL092293 e2020GL092293.